SECED 2023 Conference
Earthquake Engineering & Dynamics for a Sustainable Future
14-15 September 2023, Cambridge, UK

DEVELOPING AN INNOVATIVE REGION-WIDE RISK-INFORMED EARTHQUAKE EARLY WARNING DECISION SUPPORT SYSTEM

Yuqing LIU[1] & Gemma CREMEN[2]

Abstract: *Earthquake early warning (EEW) systems provide brief notice to targeted audiences (e.g., civil protection services) of potentially destructive seismic events. This short warning time can be used to take rapid but effective actions for reducing impending earthquake-related losses (e.g., shutting off gas supplies to prevent fires, evacuating the ground floors of buildings to mitigate casualties). Current EEW systems in use around the world do not employ risk-based metrics to support decision making for alert triggering by various end users. Instead, thresholds for issuing EEW alarms are typically based on seismological parameters (e.g., magnitude, ground-shaking intensity value) without regard for the possible consequences of triggering or not the warning. Some recent research efforts have focused on developing risk-informed EEW decision-making methodologies, but these have been limited to applications involving single assets (e.g., buildings) or specific infrastructure systems, and are not suitable for region-wide EEW. This paper addresses the limitations of state-of-the-art in EEW decision making by developing an end-user- and risk-oriented EEW decision support system (EEW DSS) for a building portfolio. The proposed EEW DSS combines conventional seismic risk assessment tools with a multi-criteria decision algorithm that relies on stakeholder risk preference input, and explicitly integrates necessary considerations associated with a region-wide, heterogenous set of buildings (e.g., spatially correlated ground motions, varying impacts of triggering or not the alarm for different building occupancies, etc.). The EEW DSS is tested for a series of earthquakes across a hypothetical urban system (>4,000 buildings). We find that the risk-informed magnitude threshold for alarm issuance increases with distance (as expected), and that the optimal action for a given magnitude/distance may depend on stakeholder risk preferences (consistent with previous studies). The proposed methodology has the potential to convert region-wide EEW systems into powerful people-centered loss-mitigation tools.*

Introduction

Earthquake early warning (EEW) is a pre-earthquake rapid intervention tool developed to avoid economic and life losses (Velazquez et al., 2020). The short warning time provided by EEW can be used for shutting off gas supplies to prevent fires and evacuating the ground floors of buildings to mitigate casualties, for instance (Gasparini et al., 2011). This study focuses on a key stage in EEW that involves identifying the optimal action to take (associated with triggering or not an EEW alarm/warning) for a detected incoming seismic event.

Existing EEW research efforts have focused predominantly on its seismological aspects (e.g., Cremen and Galasso, 2020; Cremen et al., 2022b). This means that thresholds for alarm issuance in current operational EEW systems are typically calibrated exclusively based on non-engineering-related metrics like magnitude (Velazquez et al., 2020) that do not fully capture the consequences of issuing or not a warning, including the implications of unnecessarily raising an alarm for a seismic event that does not cause any harm. While some studies have leveraged earthquake engineering theory to create enhanced risk-informed decision-making approaches for EEW (e.g., Iervolino, 2011), they have all focused on site-specific EEW applications like individual buildings (Cremen and Galasso, 2021) or port systems (Cremen et al., 2022a).

Our study instead centres on developing an advanced risk- (engineering-) oriented decision-support system (DSS) for region-wide EEW, which operates across city-sized areas located some distance from the earthquake epicenter (Velazquez et al., 2020). The proposed DSS integrates regional seismic risk assessment tools that capture necessary considerations associated with a heterogenous set of dispersed buildings (e.g., spatially correlated ground motions, varying impacts of triggering or not the alarm for different building occupancies, etc.). Furthermore, it incorporates a general multicriteria decision-making (MCDM) methodology that accounts for the

[1] Graduate student, UCL, London, UK
[2] Lecturer in Risk and Resilience Engineering, UCL, London, UK, g.cremen@ucl.ac.uk

relative importance of different consequences to stakeholders, facilitating for the first time an end-user-driven, risk-informed decision-making process for region-wide EEW. The proposed DSS is demonstrated for the building portfolio of a hypothetical urban system called "Tomorrowville" (Mentese et al., 2023). We specifically adopt the current urban layout of Tomorrowville (called TV0) as our case study, which consists of 4,810 buildings.

This paper is structured as follows. The methodology of the proposed EEW DSS is first described. It is then applied to TV0, investigating the optimal warning decision for a series of earthquakes with increasing magnitude that occur at specific distances from the building portfolio. The final section provides discussion on, and conclusions of, the study.

Methodology

Background

The proposed EEW DSS is a region-wide version of the EEW decision-making methodology for individual structural assets introduced by Cremen and Galasso (2021). The aim of the DSS is to determine the optimal portfolio-level EEW action to take among a set of risk-mitigation measures $\{A_i\}$ associated with triggering an alarm or no action *NA* (i.e, not triggering the alarm), for a detected incoming seismic event with uncertain characteristics. A conceptual outline of the proposed methodology is shown in Figure 1. The methodology will now be described in a step-by-step manner, emphasizing features that deviate from the procedure detailed in Cremen and Galasso (2021).

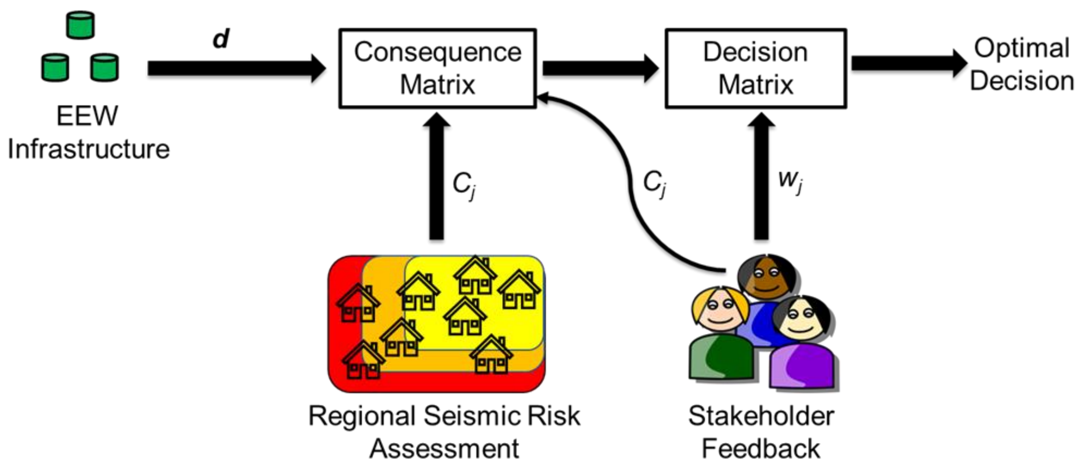

Figure 1. Conceptual outline of the proposed EEW methodology.

Step 1: Develop a consequence matrix

The purpose of this step is to characterize a prescribed set of portfolio-level consequence/loss criteria (e.g., cost, downtime) associated with $\{A_i\}$ and *NA*, conditional on the uncertain characteristics of the incoming earthquake (***d***). The value of the *j*th criterion for *NA* is equivalent to the expected value of the consequence $E^{NA}\left(C_j^{NA}\middle|\boldsymbol{d}\right)$ derived from a regional risk assessment procedure adapted to consider generic uncertainties in the earthquake characteristics, according to:

$$E^{NA}(C_j^{NA}|\boldsymbol{d}) = \iiint c_j^{NA} f\left(c_j|\boldsymbol{dm}\right) f(\boldsymbol{dm}|\boldsymbol{im}) f(\boldsymbol{im}|\boldsymbol{d}) dc_j^{NA} d\boldsymbol{dm} d\boldsymbol{im} \quad (1)$$

$f(a|b)$ is the probability density function (pdf) of *a* conditional on *b*. ***dm*** and ***im*** are portfolio-wide vector measures of damage level and ground shaking intensities, respectively. $f(\boldsymbol{dm}|\boldsymbol{im})$ is obtained using appropriate fragility functions for each building. $f(\boldsymbol{im}|\boldsymbol{d})$ is the multivariate pdf of im, given current (uncertain) information on the incoming earthquake. For this first iteration of the methodology, we assume that ***d*** contains accurate estimates of the magnitude (M^*) and epicentral distance (R_{epi}^*) of the incoming event, determined from an idealistic seismological EEW algorithm.

Thus, $f(\boldsymbol{im}|\boldsymbol{d}) = f(\boldsymbol{im}|M^*, R_{epi}^*)$, which can be computed using a ground motion model (GMM) supplemented with an appropriate spatial correlation model, for instance.

The value of the *j*th criterion for A_i $E^{A_i}\left(C_j^{A_i}\middle|\boldsymbol{d}\right)$ is a combination of the action-specific consequence associated with a false alarm $E\left(C_{ij}^{FA}\middle|\boldsymbol{d}\right)$ and the action-, criterion-, and event-specific residual amount of $E^{NA}\left(C_j^{NA}\middle|\boldsymbol{d}\right)$, denoted as $\alpha_{ij}(\boldsymbol{d})\, E^{NA}\left(C_j^{NA}\middle|\boldsymbol{d}\right)$. $E\left(C_{ij}^{FA}\middle|\boldsymbol{d}\right)$ is computed from:

$$E\left(C_{ij}^{FA}\middle|\boldsymbol{d}\right) = \sum_{k=1}^{N_b} c_{ij,k}^{FA} p(FA_k|\boldsymbol{d}) \tag{2}$$

where N_b is the number of buildings in the portfolio and $c_{ij,k}^{FA}$ is the false alarm cost for the *k*th building. $p(FA_k|\boldsymbol{d})$ is the event-dependent probability of a false alarm (i.e., no damage) occurring for the *k*th building. Each value of $E^{A_i}\left(C_j^{A_i}\middle|\boldsymbol{d}\right)$ and $E^{NA}\left(C_j^{NA}\middle|\boldsymbol{d}\right)$ are finally arranged in an $(N_A + 1) \times N_C$ matrix, as explained in Cremen and Galasso (2021), where N_A is the number of potential risk-mitigation actions and N_C is the number of considered consequence criteria.

Step 2: Develop a decision matrix

This step follows the *Technique for Order Preference by Similarity to Ideal Solution* (TOPSIS) approach to multi-criteria decision making (Yoon and Hwang, 1995), first normalizing each *i*-*j*th entry of the consequence matrix according to:

$$r_{A_i,C_j} = \frac{E^{A_i}\left(C_j^{A_i}\middle|\boldsymbol{d}\right)}{\sqrt{\sum_{i=1}^{N_A} E^{A_i}\left(C_j^{A_i}\middle|\boldsymbol{d}\right)^2 + E^{NA}\left(C_j^{NA}\middle|\boldsymbol{d}\right)^2}} \tag{3}$$

Then, the decision matrix is completed by weighting each r_{A_i,C_j} value in line with stakeholder preferences towards each criterion $\{w_j\}$, which can be captured by soliciting pairwise comparisons of each criterion according to the analytical hierarchy process (Saaty, 1980), for instance. Interested readers are referred to Cremen and Galasso (2021) for more information.

Step 2: Identify the optimal decision

This final step determines the appropriate decision to make, conditional on the current information available for the incoming earthquake, $\boldsymbol{d}$. According to the TOPSIS approach, the smallest and largest values of $r_{Ai,Cj}w_j$ (including $r_{NA,Cj}w_j$) are first identified for each criterion, which are the best (v_j^+) and worst (v_j^-) solutions for that criterion, respectively (since the criterion are negative consequences). The cumulative distances of A_i and NA from all best and worst solutions are then computed according to:

$$y_i' = \sqrt{\sum_{j=1}^{N_C} \left(v_j' - r_{Ai,Cj}w_j\right)^2} \tag{4}$$

where $y_i' = y_i^+$ or y_i^- and $v_i' = v_i^+$ or v_i^- accordingly. Finally, the optimal A_i or NA is the one with the largest S_i (or S_{NA}) value, which is determined according to:

$$S_i = \frac{y_i^-}{y_i^- + y_i^+} \tag{5}$$

Case study application to a building portfolio

Case study description

The proposed EEW DSS methodology is now demonstrated using a hypothetical 2 km × 3km virtual urban testbed called “Tomorrowville” (Mentese et al., 2023), which reflects a Global South city in terms of its physical and social characteristics. We specifically use the current urban layout of Tomorrowville (denoted as TV0), which consists of 4,810 buildings, all with known attributes related to earthquake vulnerability (including building occupancy and the number of people who use each building at peak times).

We assume that there is only one EEW-related risk-management option (*A₁*) in this case, which is simply to "Trigger the EEW alarm". The selected consequence criteria are downtime (C_1) and casualties (C_2). We explore the optimal decision among A_1 and *NA,* for a set of discrete M^* values ranging from 4.0 to 7.5 in intervals of 0.1, and corresponding R^*_{epi} values (measured from the centroid of the building portfolio) equal to 10km, 30km, and 50km from ruptures on vertical strike-slip faults. We assume that the examined earthquakes occur at 2pm on a weekday.

Step 1: Develop the consequence matrix

We generate $f(\boldsymbol{im}|M^*, R^*_{epi})$ in equation 1 at each building in TV0, using the Boore et al. (2014) global GMM with V_{S30}=500 m/s and unknown basin depths, the spatial correlation model proposed by Jayaram and Baker (2009) for clustered V_{S30} values, and 1,000 Monte Carlo simulations of the underlying probability distributions for each $\{M^*, R^*_{epi}\}$ pair (where the earthquake epicenter is assumed to be uniformly distributed on the circle with radius R^*_{epi}). $\boldsymbol{im}$ includes the intensity measures used in the fragility function for each TV0 building as detailed in Gentile et al. (2022), which are either peak ground acceleration, spectral acceleration at the building's fundamental period, or the geometric mean of spectral acceleration across a range of periods (Kohrangi et al., 2017).

In the absence of available recovery time consequence models for TV0 buildings, downtime values for each building are based on the damage-dependent building and service interruption times provided in Section 11.2.4 of Hazus (FEMA, 2020). We make the following assumptions to map TV0 buildings to Hazus occupancy classes: (1) educational facilities are assigned the "EDU1" (schools) class; (2) hospitals are assigned the "COM6" (hospital) class; (3) agricultural buildings are classified as "AGR1" (agriculture); (4) one-story residential buildings are assigned the "RES1" (single-family dwelling) class; (5) multi-story residential buildings are assigned the "RES3A-F" (multi-family dwelling) class; (6) commercial buildings are assigned the "COM4" (professional/technical/business services) class; (7) industrial buildings are assigned the "IND2" (light industrial) class; and (8) buildings within historical preservation areas are assigned the "REL1" (church) class.

C_1 values for the *NA* option are exactly equivalent to the times derived from Tables 11-8 and 11-9 of Hazus. Since these values are deterministic conditional on *dm*, equation 1 simplifies in this case to:

$$E^{NA}(C_1^{NA}|\boldsymbol{d}) = \iint C_1^{NA}(\boldsymbol{dm}) f(\boldsymbol{dm}|\boldsymbol{im}) f(\boldsymbol{im}|\boldsymbol{d})\, d\boldsymbol{dm} d\boldsymbol{im} \tag{6}$$

where $C_1^{NA}(\boldsymbol{dm}) = \sum_{k=1}^{Nb} C_{1,k}^{NA}(dm_k)$, dm_k denotes the damage level associated with the *k*th building, $C_{1,k}^{NA}(dm_k)$ is computed according to the relevant columns of Tables 11-8 and 11-9 in Hazus, and all other variables are as previously defined.

$\alpha_{11}(\boldsymbol{d})$ is based on engineering judgement, accounting for possible activities that could be implemented to reduce business and service interruption time if an EEW alarm is triggered, such as: (1) saving significant data; (2) safeguarding valuables; and (3) isolating hazardous chemical or biological systems (Allen et al., 2009). $\alpha_{11}(\boldsymbol{d})$ depends on the EEW-related mitigation effect for each *k*th individual building $\alpha_{11,k}(\boldsymbol{d})$, computed as:

$$\alpha_{11,k}(\boldsymbol{d}) = \alpha_{11,k} = 0.9 \times \delta_{11,k} \tag{7}$$

This means that the downtime values of all buildings are uniformly decreased by 10% if an EEW alarm is triggered correctly, regardless of their damage state. $\delta_{11,k} = 1$ except in the case of commercial, industrial, and hospital buildings, which are respectively assigned $\delta_{11,k} = 0.8, 0.9, \text{and } 0.9,$ to reflect additional downtime mitigation associated with saving data (commercial buildings) or avoiding leakages associated with hazardous substances (industrial/hospital buildings). Furthermore, we assume that $c_{11,k}^{FA} = 0.1$ day of disruption across all buildings, regardless of their occupancy.

At the time of occurrence of the examined earthquakes, we assume that all workers in TV0 are at their workplace, all school-going children are at school, and all other inhabitants of TV0 are at their place of residence. Furthermore, we assume that earthquake-induced casualties only occur to those who are inside each building, the total number of which is computed using the corresponding 0.7, 0.99, 0.9, and 0.9 scaling factors provided in Table 12-2 of Hazus for residential, commercial, educational, and industrial buildings respectively (note that agricultural buildings are assigned residential occupancies, per Mentese et al., 2023 and Gentile et al., 2022).

$E^{NA}(C_2^{NA}|\boldsymbol{d})$ is computed in line with equation 6, and $C_{2,k}^{NA}(dm_k)$ is derived according to:

$$C_{2,k}^{NA}(dm_k) = \sum_{m=1}^{4} CL_m(dm_k) \times N_{occ,k} \tag{8}$$

where $CL_m(dm_k)$ is the relevant damage-dependent *m*th severity-level casualty rate derived from Tables 12-3 to 12-5 of Hazus, for damage states less than complete. For the complete damage state, $CL_m(4)$ is the average of the *m*th severity-level casualty rate values according to Tables 12-6 and 12-7 of Hazus, weighted in line with the conditional probabilities of collapse provided in Table 12-8 of the document. $N_{occ,k}$ is the total number of indoor occupants in the *k*th building. TV0 buildings are mapped to Hazus structural types, as follows: (1) adobe, brick in mud, and stone in mud buildings are classified as "URML" (low-rise unreinforced masonry bearing walls); (2) brick in cement buildings are classified as "RM2L" (low-rise reinforced masonry bearing walls with concrete diaphragms); and (3) low-rise and mid-rise reinforced concrete infilled frame buildings are respectively classified as "C3L" and "C3M" (low-rise and mid-rise concrete frame with unreinforced masonry infill).

$\alpha_{12}(\boldsymbol{d})$ is computed assuming that when an EEW alarm is triggered, non-fatal casualties due to collapse are reduced by 40% (in line with Wu et al., 2012) and casualties of all severity levels in non-collapse cases are reduced by 50% (in line with Strauss & Allen, 2016). $c_{12,k}^{FA}$=0.01 in all occupied buildings, assuming a 1% probability of one casualty due to panic per Cremen et al., (2022a).

Step 2: Develop the decision matrix

The following sets of $\{w_j\}$ values are explored, to illustrate a reasonably broad variety of potential stakeholder priorities towards both consequence criteria: (1) $w_1 = w_2$= 0.5 (i.e., a stakeholder has equal preference for both criteria); (2) $w_1 =$ 0.75 and w_2= 0.25 (i.e., a stakeholder prioritizes mitigating downtime); and (3) $w_1 =$ 0.25 and w_2= 0.75 (i.e., a stakeholder prioritizes mitigating casualties).

Step 3: Identify the optimal decision

Figure 2 presents the optimal EEW decisions across the range of $\{M^*, R_{epi}^*\}$ and $\{w_j\}$ values considered.

Results and Discussion

It can be seen from Figure 2 that the magnitude threshold at which the optimal decision switches to issuing an EEW alarm increases with R_{epi}^*, regardless of the underlying stakeholder risk preferences. This is an intuitive result, arising from a combination of (1): decreasing $E^{NA}\left(C_j^{NA}\middle|\boldsymbol{d}\right)$ values at farther source-to-site distances, due to smaller ground-motion amplitudes; and (2): increasing $E\left(C_{ij}^{FA}\middle|\boldsymbol{d}\right)$ values, due to larger numbers of buildings experiencing no damage. These findings emphasise the importance of taking both event magnitude and location into account in a regional-level EEW DSS, to prevent potentially costly false alarm losses.

It is also observed from Figure 2 that stakeholder preferences can affect the optimal decision for a given $\{M^*, R_{epi}^*\}$ pair. We see that the magnitude threshold at which the optimal decision switches to issuing an EEW alarm for a given R_{epi}^* value is highest (i.e., least conservative) for the case of stakeholders placing more emphasis on minimising casualties and lowest (most conservative) for the case of stakeholders placing more emphasis on minimising downtime. An intermediate magnitude threshold is then obtained for the case of stakeholders placing equal emphasis on minimising both loss types. These findings are reasonable and can be explained by discrepancies in the relative differences between $E(C_{12}^{FA}|\boldsymbol{d})$ and $E^{NA}(C_2^{NA}|\boldsymbol{d})$ values and those between $E(C_{11}^{FA}|\boldsymbol{d})$ and $E^{NA}(C_1^{NA}|\boldsymbol{d})$. These mean that, at least for the assumptions made in this case study application, alarm-related casualty consequences dominate over those expected to be induced by the earthquake if no action is taken, for a larger magnitude range than is the case for downtime consequences. These findings, which are in line with those obtained in previous studies that have integrated MCDM into decision-making for on-site EEW applications (e.g., Cremen and Galasso, 2021; Cremen et al., 2022), underline the importance of the stakeholder engagement process in regional-level EEW alarm calibration.

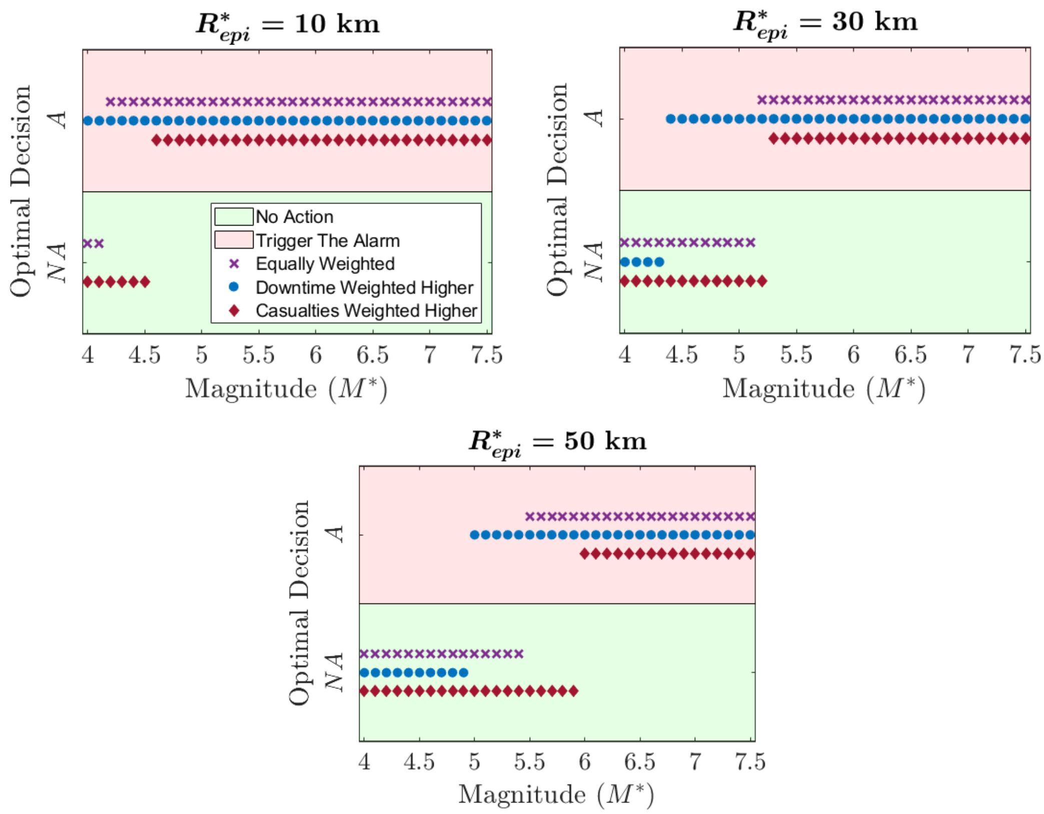

Figure 2. Identifying the optimal EEW decision across three R^*_{epi} - 10km (top left panel), 30km (top right panel), and 50km (bottom panel)- and a range of magnitudes associated with a potential incoming earthquake.

Conclusions

This work has developed and calibrated a state-of-the-art engineering-oriented region-wide EEW DSS for application to a city-level building portfolio. The DSS methodology unifies a conventional regional seismic risk assessment procedure with multi-criteria decisional tools, determining the optimal EEW-related action to take for a detected seismic event based on: (1) objectively measured consequences associated with all available actions; and (2) subjective stakeholder priorities towards different types of risk.

The case-study application of the EEW DSS to a set of more than 4,000 buildings in the Tomorrowville (TV0) virtual urban testbed clearly illustrated that the optimal EEW risk-mitigation action for a given incoming earthquake can greatly rely on stakeholders' preferences towards different types of consequences. This finding highlights the critical importance of accounting for end-user input when identifying alarm thresholds in EEW systems and is in line with the results of previous related research (e.g., Cremen & Galasso, 2021). As expected, it was found that the magnitude at which an EEW alarm should be triggered in TV0 decreases for closer epicentral distances, due to the larger amplitudes of near-source ground motion intensities.

The results of the study will facilitate better informed end-user EEW decision-making for city-level applications. Though the DSS was designed and demonstrated for a specific urban setting, it is flexible enough to be implemented within any building portfolio. The proposed algorithms can be packaged as a software plug-in to many operational EEW platforms currently in use, converting these platforms into powerful engineering-oriented end-user tools that promote thorough seismic risk mitigation. Future work will extend the methodology's capabilities by explicitly accounting for the feasibility of risk-mitigation actions as a function of available lead time and incorporating realistic dynamic source-parameter uncertainties in the risk assessment, for instance.

References

Allen RM and Melgar D (2019), Earthquake early warning: advances, scientific challenges, and societal needs, *Annual Review of Earth and Planet Sciences*, 47, 361-388.

Allen RM, Brown H, Hellweg M, Khainovski O, Lombard P, and Neuhauser D (2009), Real-time earthquake detection and hazard assessment by ElarmS across California, *Geophysical Research Letters*, 36(5).

Boore DM, Stewart JP, Seyhan E, and Atkinson GM (2014), NGA-West2 equations for predicting PGA, PGV, and 5% damped PSA for shallow crustal earthquakes, *Earthquake Spectra*, 30(3), 1057-1085.

Cremen G and Galasso C (2020), Earthquake early warning: Recent advances and perspectives, *Earth-Science Reviews*, 205, 103184.

Cremen G and Galasso C (2021), A decision-making methodology for risk-informed earthquake early warning, *Computer-Aided Civil and Infrastructure Engineering*, 36(6), 747-761.

Cremen G, Bozzoni F, Pistorio S, and Galasso C (2022a), Developing a risk-informed decision-support system for earthquake early warning at a critical seaport, *Reliability Engineering & System Safety*, 218, 108035.

Cremen G, Galasso C, and Zuccolo E (2022b), Investigating the potential effectiveness of earthquake early warning across Europe, *Nature communications*, 13(1), 1-10.

Cuéllar A, Suárez G, and Espinosa‐Aranda JM (2017), Performance evaluation of the earthquake detection and classification algorithm 2 (t S–t P) of the Seismic Alarm System of Mexico (SASMEX), *Bulletin of the Seismological Society of America*, 107(3), 1451-1463.

Eads L, Miranda E, and Lignos DG (2015), Average spectral acceleration as an intensity measure for collapse risk assessment, *Earthquake Engineering & Structural Dynamics*, 44(12), 2057-2073.

Esposito S and Iervolino I (2012), Spatial correlation of spectral acceleration in European data, *Bulletin of the Seismological Society of America*, 102(6), 2781-2788.

FEMA (2020), *Hazus 4.2: earthquake model technical manual.* Federal Emergency Management Agency (FEMA) Washington, DC.

Gasparini P, Manfredi G, and Zschau J (2011), Earthquake early warning as a tool for improving society's resilience and crisis response, *Soil Dynamics and Earthquake Engineering*, 31(2), 267-270.

Gentile R, Cremen G, Galasso C, Jenkins LT, Manandhar V, Mentese EY, Guragain R, and McCloskey J (2022), Scoring, selecting, and developing physical impact models for multi-hazard risk assessment, *International Journal of Disaster Risk Reduction*, 82, 103365.

Iervolino I (2011), Performance-based earthquake early warning, *Soil Dynamics and Earthquake Engineering*, 31(2), 209-222.

Jayaram N and Baker JW (2008), Statistical tests of the joint distribution of spectral acceleration values, *Bulletin of the Seismological Society of America*, 98(5), 2231-2243.

Jayaram N and Baker JW (2009), Correlation model for spatially distributed ground-motion intensities, *Earthquake Engineering & Structural Dynamics*, 38(15), 1687-1708.

Kohrangi M, Vamvatsikos D, and Bazzurro P (2017), Site dependence and record selection schemes for building fragility and regional loss assessment, *Earthquake Engineering & Structural Dynamics*, 46(10), 1625-1643.

Mentese EY, Cremen G, Gentile R, Filippi ME, Galasso C, and McCloskey J (2023), Future exposure modelling for risk-informed decision making in urban planning, *International Journal of Disaster Risk Reduction,* (in press).

Park J, Bazzurro P, and Baker JW (2007), Modeling spatial correlation of ground motion intensity measures for regional seismic hazard and portfolio loss estimation, *Applications of Statistics and Probability in Civil Engineering*, 1-8.

Saaty TL (1980), *The analytic hierarchy process: Planning, priority setting, resource allocation*, New York: McGraw-Hill International Book Co.

Strauss JA and Allen RM (2016), Benefits and costs of earthquake early warning, *Seismological Research Letters*, 87(3), 765-772.

Velazquez O, Pescaroli G, Cremen G, and Galasso C (2020), A review of the technical and socio-organizational components of earthquake early warning systems, *Frontiers in Earth Science*, 445.

Wang C, Cremen G, Gentile R, and Galasso C (2022), Design and assessment of pro-poor financial soft policies for expanding cities, *International Journal of Disaster Risk Reduction*, 85(1), 103500.

Wu S, Beck JL, and Heaton TH (2012), Decision criteria for earthquake early warning applications, *Proceedings of the 15th World Conference of Earthquake Engineering, Lisbon, Portugal* (No. 0973).

Yoon,KP and Hwang CL (1995), *Multiple attribute decision making: An introduction*., London, New Dehli: Sage Publications.